Journal of Machine Engineering, Vol. 16, No. 1, 2016

Received: *11 January 2016* / Accepted: *16 February* / Published online: *10 March 2016*

machine tools, robustness,
uncertainty, artefact,

Md Mizanur RAHMAN[1*]
Rene MAYER[1]

CALIBRATION PERFORMANCE INVESTIGATION OF AN UNCALIBRATED INDIGENOUS ARTEFACT PROBING FOR FIVE-AXIS MACHINE TOOL

On machine measurement of artefacts such as single ball, multiple balls or even prismatic shape artefact is gaining popularity for the calibration of five-axis machine tools. However, calibration results can be degraded due to errors from different process variables such as the measurement strategies, rotary axes indexations and artefact dismount and remount cycles. This research investigates the repeatability of uncalibrated indigenous artefact probing and machine tool error parameters calibration against a number of process variables. Uncertainties of the estimated parameters are estimated to quantify the calibration quality.

1. INTRODUCTION

FIVE-AXIS MACHINE TOOLS offer numerous opportunities to produce complex parts because of their ability to orient the tool with respect to the workpiece. Due to the existence of two rotary axes, direct calibration, such as laser interferometry, are difficult, time consuming, require trained personnel and are sometimes complicated to implement. In contrast, indirect calibration techniques are comparatively easy to adapt and can often be automated [1]. Since CNC machine tools are usually equipped with a touch trigger probe, some researchers have developed indirect calibration technique involving the measurement of different artefacts to gather machine tools geometric information. Hence, the measuring capability of the machine tool becomes a prior concern.

In [1],[2],[3],[4],[5],[6], much work is presented to estimate geometric and dynamic error parameters for CNC machine tools using indirect approaches but the variability of these approaches against process variables has not been addressed except for Verma et al. [12] whom investigated the influence of the most significant variable on the measurement accuracy of a CNC machine tool and found that tool change and machine tool warm up cycles are major contributors.

Some research [7],[8],[9],[10],[11],[12] considered the measurement inaccuracies introduced by the measuring instruments (touch trigger probe etc.) for Coordinate Measuring Machines (CMMs) and CNCs with detail error modelling.

[1] Mechanical Engineering Dept., Polytechnique Montréal, Montréal (QC), Canada
[*] E-mail: mdmizanur.rahman@polymtl.ca

Machine tool's moving parts such as: bearings, gear and hydraulic oil, drives and clutches, pumps and motors, guideways, cutting action and swarf, external heat sources etc. generate heat while the machine tool is in continuous operation [13]. Martin et al. found that over 50% of the overall machine tool inaccuracy was caused by these internal or external heat sources. They proposed a thermal error compensation model where the displacement of the tool center point (TCP) can be calculated by a transfer function (TF) that contains models based on heat transfer principles. The TF modeling approach was applied to different machine tools with similar components and structures but different initial expansion in individual parts. The improvement was 87% compared to the uncompensated state. The improvement in calibration performance between the machine tools varies only 1% which implies the TF model's portability among variety of machine tools [14]. Jerzy and Wojciech reviewed the integration of intelligent functions such as active vibration control, intelligent thermal shield, safety shield, voice adviser, intelligent performance spindle, maintenance support and balance analyser in machine tools in order to make them autonomous (self supervision, self diagnosis, etc.). For high performance machine tools, the authors implicate the importance to holistic modeling and numerical simulation of machine tool's operational properties during the entire machining process in order to enhance the capabilities and effectiveness of identifying and minimizing the disturbance and error compensation. They concluded that integrating these intelligent functions will increase efficiency and precision while minimizing production costs [15].

Authors investigated the influence of machine tools status change during a day period and between consecutive days on the calibration performance of an on-machine probing of an uncalibrated indigenous artefact on a five-axis machine tool [16]. This research investigates the influence of variables such as the measurement strategy, rotary axes indexations and artefact dismount and remount cycles on the performance of calibration. Uncertainty estimates of the calibrated parameters will be considered for this analysis.

2. MATHEMATICAL BACKGROUND

A similar artefact probing strategy to those described in [1] is used where facets are probed based on their nominal position and nominal local normals. Homogeneous transformation matrices (HTMs) transform axis command into the position of the stylus tip with respect to the facets from which linear equations are produced in order to estimate the error parameters.

$$\boldsymbol{\delta d} = \boldsymbol{J} \cdot \boldsymbol{\delta E} \tag{1}$$

Where, δd are the distance between facets and stylus tip calculated using the nominal model, J is the Jacobian sensitivity matrix of the facets to stylus tip for small change is distances and δE are the estimated error parameters. In this study, inter-axis errors, scale gains and backlash will be estimated. For the parameter uncertainty estimation, GUM uncertainty framework (GUF) is used. The estimation process is based on a multi-input and multi-output model and the covariance of the input quantities is required [16]. For an output quantity $\boldsymbol{Y} = (Y_{1,}\ldots, Y_{\mathrm{m}})^{\mathrm{T}}$ and an input quantity $\boldsymbol{X} = (X_{1,}\ldots, X_{\mathrm{N}})^{\mathrm{T}}$, with

$$\boldsymbol{Y} = \boldsymbol{f}\,(\boldsymbol{X}) \tag{2}$$

where $f = (f_1, \ldots, f_{\mathrm{m}})^{\mathrm{T}}$.

Then, the output uncertainties, as a covariance matrix, can be calculated using the following formula [17]

$$\boldsymbol{U_y} = \boldsymbol{C_x}\boldsymbol{U_x}\boldsymbol{C_x^{\mathrm{T}}} \tag{3}$$

3. CALIBRATION PERFORMANCE ANALYSIS

In this section, performance of the indirect calibration technique by probing an indigenous artefact is investigated against probing strategies, change in machine tool status during a day and between consecutive days, artefact dismount and remount cycle and rotary axis indexations.

3.1. INFLUENCE OF THE PROBING STRATEGIES

Calibration was done for four different probing strategies while the rotary axes indexations remains the same but the facets location was changed. The total number of 251 probing points remains the same for all the strategies. A particular strategy is conducted during a specific day. Each day has a different strategy. There are four strategies and so four days of test. So, for four consecutive days, each strategy repeats for four cycles each day as shown in Table 1. The time required for four repeated cycles is 6 h 6 min. for each strategy hence each cycle takes approximately 1 h 30 min.

Table 1. Effect of strategies: Analysis criteria

Four repeated cycles per strategy					Strategy-wise analysis
Day-1, Strategy 1	Cycle 1	Cycle 2	Cycle 3	Cycle 4	Mean values of the estimated parameters at each strategy for four repeated cycles
Day-2, Strategy 2	Cycle 1	Cycle 2	Cycle 3	Cycle 4	
Day-3: Strategy 3	Cycle 1	Cycle 2	Cycle 3	Cycle 4	
Day-4, Strategy 4	Cycle 1	Cycle 2	Cycle 3	Cycle 4	

In order to observe the effect of the strategies, the means of the estimated parameters for four repeated cycles at each strategy are calculated and compared (Table 1). Results are shown in Table 2. The overall mean of the parameters for all the strategies has also been calculated and compared with the mean of the individual strategies.

Table 2. Effect of change in probing strategy (change in facets location). Mean values of the estimated parameters of all strategies, individual strategy and the range of means of the strategies

Strategy-wise mean values						
Estimated Parameters	Overall mean (all strategies)	Day 1	Day 2	Day 3	Day 4	Range of means
		Strategy 1	Strategy 2	Strategy 3	Strategy 4	
E_{XXb} (µm)	5.82	5.18	6.16	5.38	5.65	0.98
E_{AOB} (µrad)	-36.51	-41.15	-38.06	-36.98	-33.78	7.37
E_{COB} (µrad)	-7.35	-6.57	-7.37	-6.51	-9.65	3.14
E_{XOS} (µm)	-132.87	-125.83	-128.00	-128.08	-127.23	2.25
E_{YOS} (µm)	24.51	26.08	25.02	24.48	24.89	1.59
E_{YY} (µm/m)	-29.86	-26.42	-28.91	-27.42	-27.62	2.49
E_{YYb} (µm)	-5.92	-6.33	-5.62	-5.58	-5.48	0.85
E_{BOZ} (µrad)	84.96	63.40	66.98	67.11	64.51	3.71
E_{ZZ} (µm/m)	-52.12	-52.19	-57.42	-56.55	-51.00	6.42
E_{AOY} (µrad)	-17.27	-22.03	-21.28	-15.45	-16.25	6.58
E_{COY} (µrad)	14.79	13.50	15.19	15.08	14.54	1.70
E_{XOC} (µm)	-109.10	-109.43	-109.59	-110.10	-110.19	0.76
E_{AOC} (µrad)	8.78	-3.38	-4.80	-1.88	-8.78	6.90
E_{BOC} (µrad)	11.58	5.46	5.89	6.69	5.76	1.23
E_{BBb} (µrad)	8.93	7.99	8.88	8.43	8.89	0.90
E_{CCb} (µrad)	-0.19	-0.22	0.57	-0.69	-0.48	1.26
E_{XX} (µm/m)	-9.89	-7.18	-10.05	-10.25	-8.82	3.07

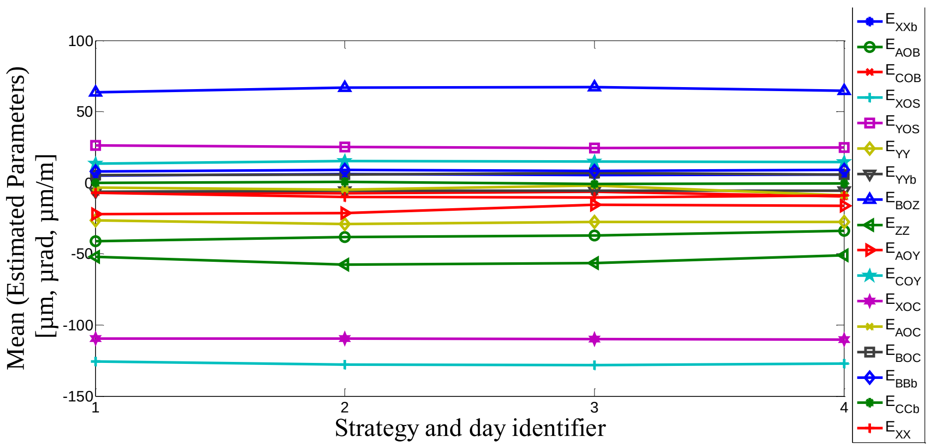

Fig. 1. Effect of change in probing strategy (change in facets location). Mean values of the estimated parameters of all strategies

Table 2 shows the overall mean, strategywise mean and the range of means for different strategies of the estimated parameters while

Fig. 1 shows the change in mean values throughout the strategies. Result shows that, E_{A0B}, E_{ZZ}, E_{AOY} and E_{AOC} have noticeable variation in range of means otherwise the range of mean values of the parameters at different strategies are considerably smaller.

3.2. INFLUENCE OF ARTEFACT DISMOUNT AND REMOUNT CYCLE

The artefact used in this work is the original machine tool table. In this section, the effect of artefact dismount and remount on the parameters estimation is analysed. The machine tool undergoes three different phases. The warmup phase is approximately two hours from the machine tool cold condition and no measurements has been done in this phase, then the first measurement cycle is ran before artefact change followed by a second measurement cycle. Each measurement cycle takes approximately 1 h 30 min. During artefact change, the artefact is dismounted and put back into the machine tool's table depot then brought back and remounted again in the machine tool workspace. These operations are automated. The artefact dismount and remount cycle takes 3 min 30 sec. approximately. This procedure was repeated the following day and the results are given in Table 3.

Table 3. Effect of artefact dismount and remount cycle in parameter estimation

	Day 1	Day 2		Day 1	Day 2		
Estimated Parameters	Before artefact change	Before artefact change	Range	After artefact change	After artefact change	Range	ΔRange
E_{XXb} (μm)	4.68	9.30	4.62	4.28	6.40	2.12	2.5
E_{AOB} (μrad)	-55.16	-47.78	7.38	-45.15	-40.16	4.99	2.39
E_{COB} (μrad)	-0.80	-5.84	5.04	-3.47	-5.85	2.38	2.66
E_{XOS} (μm)	-130.98	-127.83	3.15	-130.42	-132.57	2.15	1
E_{YOS} (μm)	30.25	25.08	5.17	26.89	23.97	2.92	2.25
E_{YY} (μm/m)	-25.04	-36.46	11.42	-12.58	-22.78	10.2	1.22
E_{YYb} (μm)	-5.82	-3.53	2.29	-4.98	-3.91	1.07	1.22
E_{BOZ} (μrad)	71.75	63.88	7.87	66.06	69.75	3.69	4.18
E_{ZZ} (μm/m)	-60.44	-66.75	6.31	-50.77	-55.64	4.87	1.44
E_{AOY} (μrad)	-34.29	-35.35	1.06	-22.53	-23.93	1.4	0.34
E_{COY} (μrad)	20.58	17.59	2.99	16.94	15.44	1.5	1.49
E_{XOC} (μm)	-105.42	-102.84	2.58	-104.70	-105.01	0.31	2.27
E_{AOC} (μrad)	-3.65	-7.60	3.95	-2.16	-5.44	3.28	0.67
E_{BOC} (μrad)	16.98	16.62	0.36	16.59	16.69	0.1	0.26
E_{BBb} (μrad)	8.49	7.96	0.53	7.32	7.17	0.15	0.38
E_{CCb} (μrad)	2.42	2.24	0.18	0.29	1.80	1.51	1.33
E_{XX} (μm/m)	-7.37	-6.56	0.81	0.01	-1.64	1.65	0.84

Result shows that artefact mount dismount cycle has no significant effect. This is expected for two reasons. One is that the mechanism for table mounting was found to be relatively repeatable, and the other reason is that the mathematical model includes the artefact and tool setup errors as separately estimated variables. The test is affected by variability due to the change between the cycles during a day period and change between days for consecutive days as described in authors' previous work [16].

3.3. INFLUENCE OF ROTARY AXES INDEXATIONS CHANGE

Measuring an artefact at different rotary axes indexation provides rich information about the machine tools geometry. But change in probing strategy by changing the number of rotary axes indexations may affect the parameters estimation. Since the artefact is measured at every rotary axes combination hence the higher the number of rotary axes combination the more measurement points are gathered. However, this also means more non-productive time for the machine tool so it is worth investigating the effect of increasing the number of indexations in the strategy on the estimated error parameters. For this purpose, a particularly rich probing strategy was repeated five times per day for four consecutive days. The probing strategy includes 28 combinations of Spindle-B-C (ABC) axes indexations. Out of these 28 indexations, five different subsets of ABC indexations have been chosen to evaluate the influence of rotary axes indexation on parameter estimation. The subsets are chosen based on the condition number of the Jacobian matrix by simulating the measurement subsets.

The condition number is a mathematical quantity to determine the numerical quality of the estimation. A low condition number provide better estimates. In this investigation, more than 10 different measurement strategies were analyzed with different ABC subsets and found that measurement strategy with higher number of ABC indexations does not necessarily means better estimates. Five indexation subsets are selected for this analysis.

Table 4. Condition number for different ABC indexation sets

	ABC sets					
	Complete ABC sets	Subset 1	Subset 2	Subset 3	Subset 4	Subset 5
	28	23	24	25	22	21
Condition Number	10073	10011	9143	9678	9230	8975

Table 4 shows the condition number of the selected ABC indexation subsets. During the simulation, 17 machine error parameters are included in the model as shown in Table 2. The selected subsets have been applied to the 20 measurement cycles (five cycles per day for four consecutive days). The standard deviations of the estimated parameters for each subset are calculated, mean and range of the standard deviations are also calculated and given in Table 8. Fig. 2 shows the mean values of the estimated parameters for the five subsets.

From Fig. 2 it is observed that the mean values for the subsets have similar trends in terms of parameter values. E_{B0Z} and E_{ZZ} has noticeable amount of standard deviation while others are significantly smaller (around or below 5 µm, µrad or µm/m). E_{XX} and E_{X0C} are the most stable parameters.

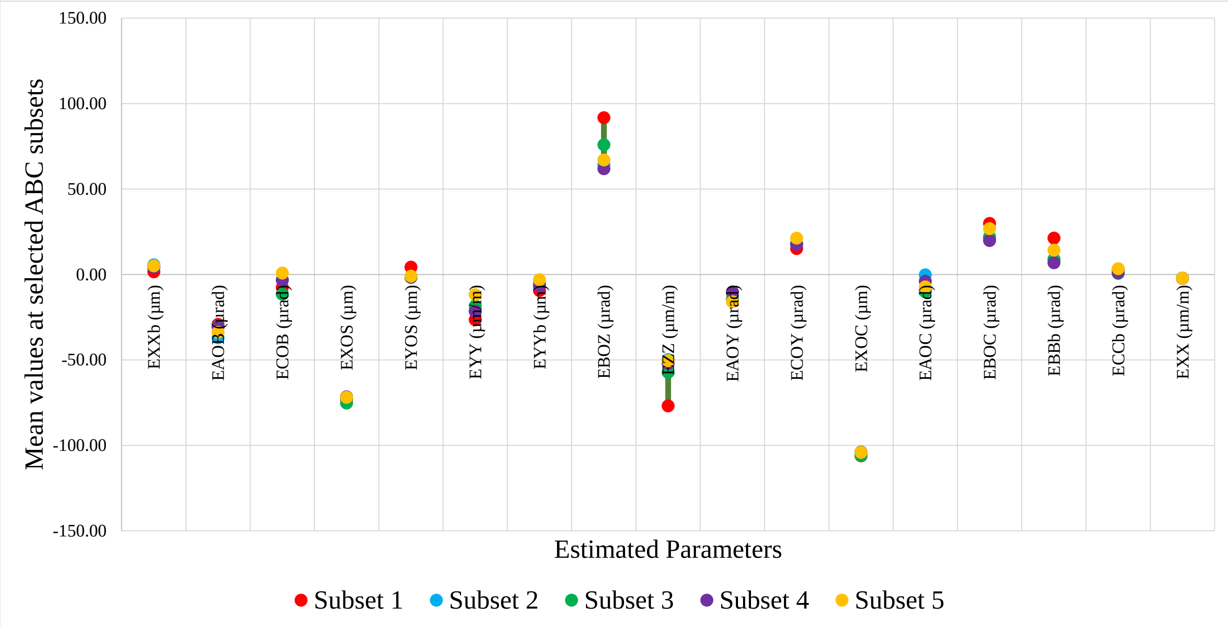

Fig. 2. Mean values of the estimated parameters for the five ABC subsets applied to the 20 measurement cycles

Table 5. Mean and standard deviations of the estimated parameters for the five ABC subsets applied to the 20 measurement cycles

	Subset 1 (23 ABC sets)	Subset 2 (24 ABC sets)	Subset 3 (25 ABC sets)	Subset 4 (22 ABC sets)	Subset 5 (21 ABC sets)	Standard Deviations
E_{XXb} (µm)	1.47	5.55	4.80	4.04	4.93	1.43
E_{AOB} (µrad)	-29.31	-37.04	-30.27	-30.60	-33.91	2.86
E_{COB} (µrad)	-7.59	-3.19	-11.59	-3.37	0.76	4.22
E_{XOS} (µm)	-73.13	-72.04	-75.28	-71.64	-71.87	1.35
E_{YOS} (µm)	4.25	-1.40	-1.74	-1.56	-1.12	2.29
E_{YY} (µm/m)	-26.49	-21.28	-18.44	-21.59	-11.86	4.80
E_{YYb} (µm)	-9.44	-5.28	-5.28	-6.86	-3.12	2.09
E_{BOZ} (µrad)	91.66	64.11	75.82	61.82	66.95	10.88
E_{ZZ} (µm/m)	-76.95	-49.88	-57.33	-52.04	-50.48	10.15
E_{AOY} (µrad)	-10.55	-15.35	-14.35	-10.22	-15.97	2.43
E_{COY} (µrad)	15.13	17.81	17.90	17.51	21.21	1.94
E_{XOC} (µm)	-106.12	-104.76	-105.96	-103.95	-104.16	0.90
E_{AOC} (µrad)	-9.09	-0.27	-10.15	-3.99	-7.25	3.61
E_{BOC} (µrad)	29.80	22.13	21.40	19.81	26.75	3.72
E_{BBb} (µrad)	21.23	8.92	8.58	6.82	14.16	5.25
E_{CCb} (µrad)	3.00	1.86	0.52	1.04	3.28	1.07
E_{XX} (µm/m)	-2.24	-2.23	-2.24	-2.23	-2.23	0.01

3.4. UNCERTAINTIES OF THE ESTIMATED PARAMETERS

Uncertainties of the estimated parameters were estimated using a covariance matrix generated from the measurement data obtained from the five repeated measurement cycles of a particular measurement strategy for four consecutive days. The uncertainty values are given in Table 6.

Table 6. Uncertainties of the estimated parameters

Parameters' names	E_{XXb} (μm)	E_{AOB} (μrad)	E_{COB} (μrad)	E_{XOS} (μm)	E_{YOS} (μm)	E_{YY} (μm/m)	E_{YYb} (μm)	E_{BOZ} (μrad)	E_{ZZ} (μm/m)
Uncertainties	2.22	2.43	1.42	3.28	1.07	5.16	0.87	4.51	5.18
Parameters' names	E_{AOY} (μrad)	E_{COY} (μrad)	E_{XOC} (μm)	E_{AOC} (μrad)	E_{BOC} (μrad)	E_{BBb} (μrad)	E_{CCb} (μrad)	E_{XX} (μm/m)	
Uncertainties	3.18	1.63	0.86	1.41	7.49	0.56	0.85	3.28	

Results shows that C-axis out of squareness to X-axis (E_{BOC}), Y- and Z-axis scale gains (E_{YY} and E_{ZZ}) and Z-axis out of squareness to X-axis (E_{B0Z}) have noticeably higher uncertainty values. Fig. 3 shows the uncertainties versus standard deviations obtained in section 0. Similar trends are observed between the standard deviation and uncertainties but the uncertainties are always larger.

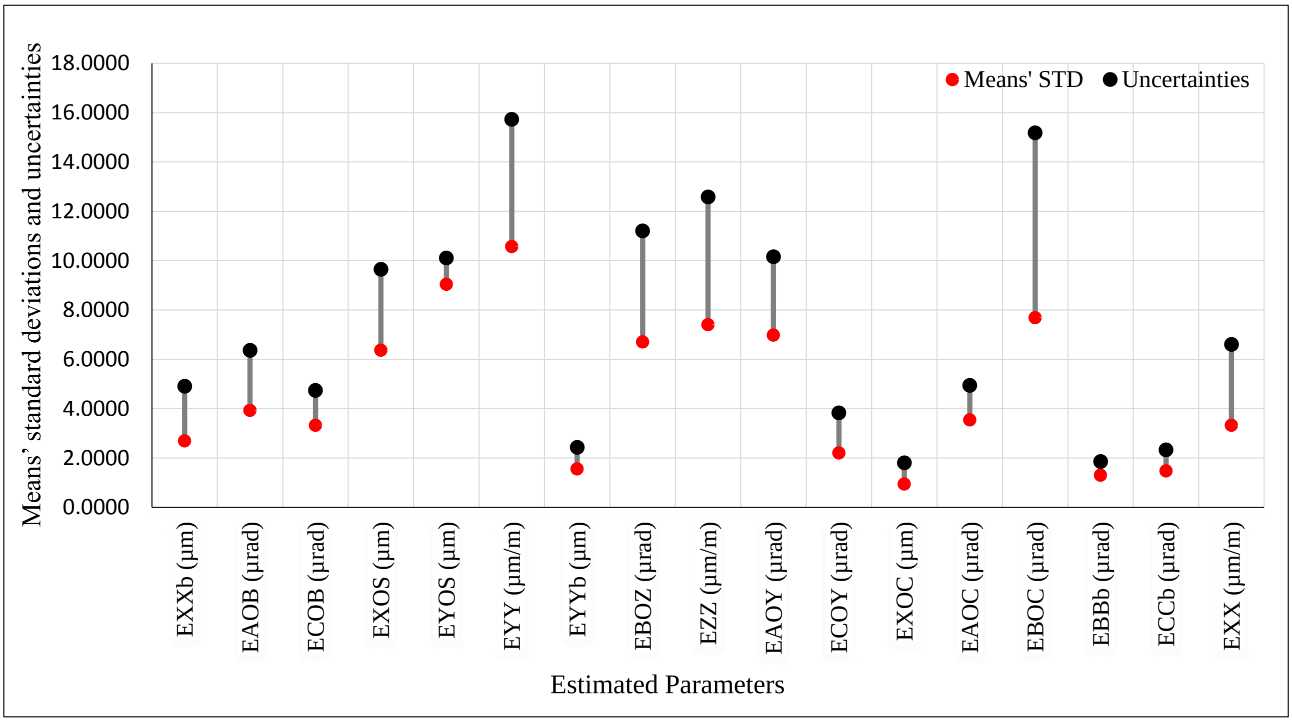

Fig. 3. Uncertainties vs standard deviation of the estimated parameters

4. CONCLUSION

Performance of an indirect calibration technique by probing an indigenous artefact against some measurement process variables has been investigated in this work. Result shows that E_{A0B}, E_{ZZ}, E_{A0Y} and E_{A0C} are influenced by change in measurement strategy with ranges of 7.37 µrad, 6.42 µm/m, 6.58 µrad and 6.9 µrad while others are around or below 3 (µrad, µm or µm/m). As expected, the artefact dismount and remount cycle does not have significant effects on the estimation since this effect is considered in the estimation process. The selection of measurement strategy in terms of rotary axes indexation combinations plays an important role in calibration. The strategy can be optimized by observing the condition number which can reduce the time of the measurements. Standard deviation of the estimated parameters obtained for the indexation subsets are below the uncertainties. E_{B0C}, E_{YY}, E_{B0Z} and E_{ZZ} have noticeably higher standard deviation and uncertainties.

ACKNOWLEDGMENTS

Work funded by NSERC, CRIAQ, Pratt & Whitney Canada, Meloche Group and SONACA Montreal. Authors are grateful for the experimental support of G. Gironne and V. Mayer.

REFERENCES

[1] RAHMAN M.M., MAYER J.R.R., 2014, *Five axis machine tool volumetric error prediction through an indirect estimation of intra and inter axis error parameters by probing facets on a scale enriched uncalibrated indigenous artefact*, Precision Engineering, 40, 94-105.

[2] SCHWENKE H., KNAPP W., HAITJEMA H., WECKENMANN A., SCHMITT R., DELBRESSINE F., 2008, *Geometric error measurement and compensation of machines—An update*, CIRP Annals - Manufacturing Technology, 57/2, 660-675.

[3] ERKAN T., MAYER J.R.R., DUPONT Y., 2011, *Volumetric distortion assessment of a five-axis machine by probing a 3D reconfigurable uncalibrated master ball artefact*, Precision Engineering, 35/1, 116-125.

[4] MAYER J.R.R., 2012, *Five-axis machine tool calibration by probing a scale enriched reconfigurable uncalibrated master balls artefact*, CIRP Annals - Manufacturing Technology, 61/1, 515-518.

[5] WEIKERT S., KNAPP W., 2004, *R-test, a new device for accuracy measurements on five axis machine tools*, CIRP Annals - Manufacturing Technology, 53/1, 429-432.

[6] IBARAKI S., IRITANI T., MATSUSHITA T., 2012, *Calibration of location errors of rotary axes on five-axis machine tools by on-the-machine measurement using a touch-trigger probe*, International Journal of Machine Tools and Manufacture, 58, 44-53.

[7] CAUCHICK-MIGUEL P.A., KINGS T.G., 1998, *Factors which influence CMM touch trigger probe performance*, International Journal of Machine Tools and Manufacture, 38/4, 363-374.

[8] WOZNIAK A., DOBOSZ M., 2005, *Factors influencing probing accuracy of a coordinate measuring machine*, IEEE Transactions on Instrumentation and Measurement, 54/6, 2540-2548.

[9] JOHNSON R.P., QINGPING Y., BUTLER C., 1998, *Dynamic error characteristics of touch trigger probes fitted to coordinate measuring machines*, Proc. IMTC/98 Conference. IEEE Instrumentation and Measurement Technology Conference. Where Instrumentation is going (Cat. No.98CH36222), 18-21 May 1998, IEEE, 1168-1172

[10] JANKOWSKI M., WOZNIAK A., BYSZEWSKI M., 2014, *Machine tool probes testing using a moving inner hemispherical master artefact*, Precision Engineering, 38/2, 421-427.

[11] JANKOWSKI M., WOZNIAK A., 2016, *Mechanical model of errors of probes for numerical controlled machine tools*, Measurement: Journal of the International Measurement Confederation, 77, 317-326.

[12] VERMA M.R., CHATZIVAGIANNIS E., JONES D., MAROPOULOS P.G., 2014, *Comparison of the measurement performance of high precision multi-axis metal cutting machine tools*, Proc. International Conference on Digital Enterprise Technology - DET 2014 Disruptive Innovation in Manufacturing Engineering towards the 4th Industrial Revolution, 25- 28 March 2014, Elsevier, 138-145.

[13] RAMESH R., MANNAN M.A., POO A.N., 2000, *Error compensation in machine tools - a review. Part II: Thermal errors*, International Journal of Machine Tools and Manufacture, 40/9, 1257-1284.

[14] MARES M., HOREJS O., HORNYCH J., SMOLIK J., 2013, *Robustness and portability of machine tool thermal error compensation model based on control of participating thermal sources*, Journal of Machine Engineering, 13/1, 24-36.

[15] JEDRZEJEWSKI J., KWASNY W., 2015, *Development Of Machine Tool Operational Properties*. Journal of Machine Engineering, 15/1, 5-24.

[16] MAYER J.R.R., RAHMAN M.M., LOS A., 2015, *An uncalibrated cylindrical indigenous artefact for measuring inter-axis errors of a five-axis machine tool*, CIRP Annals- Manufacturing Technology, 64/1, 487-490.

[17] JCGM, 102, 2011, Evaluation of measurement data – Supplement 2 to the “Guide to the expression of uncertainty in measurement” – Extension to any number of output quantities," GUM uncertainty framework.